



AERODYNAMIC CHARACTERISTICS OF TWO DIFFERENT AIRFOILS USING PANEL METHOD

Nabeel Mohammed Jasim

University of Kufa / Mechanical Engineering Department

Received:23/1/2010 ;Accepted :13/6/2010)

Abstract :

In this paper, a numerical investigation to analysis the potential flow over 2D airfoil, is carried out. The governing equation for potential flow is Laplace's equation, a widely studied linear partial differential equation. One of Green's theorem can be used to write a solution to Laplace's equation in a two-dimensional domain subjected to the Neumann boundary condition using Panel method. A computer program is developed by implementing a specific model using doublet panels of constant strength to compute the flow over a member of two different airfoil shapes (NACA0020 & NACA4412). The results are presented in terms of streamlines to show the behavior of the fluid flow for several values of angle of attack ($\alpha = 0^\circ, 5^\circ, \text{ and } 10^\circ$). Also, pressure distribution, lift coefficient, pitching moment, and drag coefficient are calculated for the airfoils. The results show that the pressure distribution, lift coefficient, pitching moment, and drag coefficient are a strong function of the airfoil's geometry and the angle of attack. Also the peak value of the lift coefficient for NACA4412 is observed to occur at angle of attack of (10°) and its value is equal to (1.82), while its value is equal to (0.9) for NACA0020 at the same value of angle of attack. The numerical results of lift coefficient have been confirmed by comparing it with experimental and other numerical results. Good agreement was obtained.

Keywords : potential flow, airfoil, panel method, pressure distribution, aerodynamics.

الخلاصة :

في هذا البحث تم إجراء دراسة عددية لتحليل الجريان الجهدي (الجريان بالطاقة الكامنة) حول جناح ثنائي البعد. إن المعادلة الحاكمة للجريان الجهدي هي معادلة لابلاس (لابلاس) والتي تعتبر من المعادلات التفاضلية الجزئية الخطية التي تدرس على نطاق واسع. وقد تم حل معادلة لابلاس حسب نظرية (كرين) في مجال ثنائي البعد يخضع لشروط (نيومان) الحدية و باستخدام طريقة اللوحة أو الأجزاء. تم إنشاء برنامج حاسوبي بالاعتماد على الموديل الرياضي المستخدم و حسب طريقة القيمة الثابتة لمعامل دوبلت لكل لوحة لغرض تحليل الجريان حول شكلين مختلفين من الجناح (NACA0020 & NACA4412). تم تمثيل نتائج الدراسة بدلالة خطوط الانسياب لبيان سلوك الجريان و لقيم مختلفة من زاوية الجريان ($\alpha = 0^\circ, 5^\circ, \text{ and } 10^\circ$). كذلك تم حساب و إيجاد توزيع الضغط، و معاملات الرفع، العزم و السحب للجناح. لقد بينت النتائج بان توزيع الضغط، و معاملات الرفع، العزم و السحب هي دالة قوية لشكل الجناح و زاوية الجريان. كذلك بينت النتائج أن القيمة القصوى لمعامل الرفع للجناح (NACA4412) تحدث عند زاوية جريان (10°) و قيمته تساوي (1.82)، في حين أن قيمته تساوي (0.9) للجناح (NACA0020) عند القيمة نفسها لزاوية الجريان. لقد تم مقارنة النتائج العددية لقيم معامل الرفع لهذه الدراسة مع نتائج عملية و عددية لدراسات سابقة و وجد إن الحل العددي الحالي مقارب جدا لهذه الدراسات.

Nomenclature:

Symbol	Description	Unit
c	Airfoil chord	m
C_L	Lift coefficient	-
C_m	Pitching moment coefficient	-
C_p	Pressure coefficient	-
N	Number of panels	-
S	Total boundary surface of the fluid domain	-
S_B	body with unknown boundaries	-
S_w	Wake surface	-
U_∞	Velocity of fluid partials	m/s
u, v	Velocity components in x, y direction,	m/s
u_p, v_p	Velocity components in panel coordinates	m/s
x, y	Cartesian coordinates	m
x_o, y_o	The coordinates of the panel origin	m

Greek symbols:

α	Angle of attack	Degree
Γ	Circulation	m ² /s
μ	Doublet strength	-
σ	Source strength	-
ϕ	Perturbation velocity potential	-
ϕ_∞	Free stream potential	-
ϕ_t	Total tangential velocity	-
∇	Gradient operator	-

Subscript:

o	Original coordinates	-
P	Panel coordinates	-
∞	Conditions far from the airfoil	-

1- Introduction :

Due to the advances needed for high aerospace performance, a legitimate need for accurate aerodynamic estimates has arisen. Also, availability of detailed accurate aerodynamic data (e.g. detailed pressure distribution) is considered a necessary input for the detailed structure design and body thickness distribution, consequently, weight savings can be achieved which is an essential task in aerospace demands, [Hess 1990].

To solve the problem of potential flow over a solid object, Laplace's equation must be solved subject to the boundary condition that there be no flow across the surface of the object. One of Green's identities can be used to write a solution to Laplace's equation as a boundary integral.

Hess and Smith (1964), laid the foundation for the source panel method. The idea of the vortex panel method is due to Martensen (1971), and is extended by Lewis (1991). Morino, Chen, and Suciu (1975), developed a method to calculate the steady and oscillatory subsonic and supersonic aerodynamics around complex configurations. The method was applied to the analysis of the flow field around wings and wing –body combination. Good results were obtained for wing –body combination in steady flow and for finite-thickness wings in oscillatory flow. Raj and Gray (1978), used a linear-varying vortex surface distribution and zero-normal flow B.C. in computation of two-dimensional potential flow. The agreement of the computed results with ones obtained by conformal transformation technique was mostly within 1 %. Asfar, Mook, and Nayfeh (1979), presented a numerical technique that predicts the potential flow field past arbitrary bodies. A combination of a vortex lattice and sources was done to represent the body surface. Chen and Sheu (1989), presented a number of integral equation methods, including internal and surface singularity methods to calculate the two – dimensional potential flow around multi element airfoils. Two and three element airfoils were used in the study. The study showed that; some of both the internal and surface singularity methods can be used. Yon (1990), performs an extensive study of nine different panel methods and reports finally that the combined constant source and doublet method with the Dirichlet formulation is the most robust from the practical requirements of speed and least sensitivity to panel densities.. Albano and Rodden (1991), used a doublet lattice method for calculating lift distributions on oscillating surfaces in subsonic flows. They developed an approximate method from the linearized formulation by idealizing the surface as a set of lifting elements, which were small trapezoidal panels arranged in columns parallel to the free stream. The normal velocity induced by an element of unit strength was given by an integral of the subsonic kernel function. Results for two and three dimensional flows were outlined. Hess (1991), analyzed and tested the ability of use of higher-order surface singularity distributions to obtain improved

potential flow solutions for two dimensional Neumann problem. The study documented that; fairly accurate pressure distributions can be obtained on most airfoils using about 20 elements, especially if the higher-order method is used with a parabolic vorticity variation. Al-baldiwe (1997), developed an approximate approach to calculate the flow around small aspect ratio wing-body combination. A doublet – vortex method was suggested and developed in order to estimate the influence of a circular cross-sectional body on a flat plate wing. Sakir (1999), described the potential-based panel method for the hydrodynamic analysis of 2-D hydrofoils moving under a free surface with constant speed without consideration of the cavitation phenomenon using Dirichlet boundary condition. The study examined the effect of free surface by a parametric variation of the Froude number and depth of submergence. Katz and Plotkin (2001), give a comprehensive overview of panel methods in general. Aimen (2001), used the panel method to study the solutions for potential flows past thick and thin symmetrical and nonsymmetrical bodies and then compared with either the exact analytical methods solution or the solution obtained by using a perturbation method. All of those researchers used the panel method in their researches, they divided the body surface into small panels and distributed elementary solutions on each panel but, the differences between them were the discretization of the geometry (the use of flat or non-flat panels) and the discretization of the elementary solution distribution (the use of constant, linear-varying, and quadratic-varying strength elementary solution distribution).

The aim of this work is to study numerically the potential flow over two dimensional airfoil with two different shapes (NACA0020 & NACA4412) subjected to the Neumann boundary condition using panel method. The influences of angle of attack on the flow fields (streamlines), pressure distribution, lift, moment, and drag coefficients is examined. To give good indication about the influence of system parameters, results were formulated using modern techniques and presented in detailed using Excel and Surfer software. These results document the dependence of lift, moment, and drag coefficients on the governing parameters (angle of attack and airfoil geometry).

2- Mathematical Formulation :

Consider a steady uniform flow past a fixed 2-D airfoil. The airfoil configuration and coordinate system of the problem under consideration are depicted in Fig. (1). The (x-y) Cartesian coordinate system is chosen. At low speeds, it is assumed that the fluid is incompressible, inviscid and that the flow far from the airfoil is irrotational. Thus, the steady 2-D flow can be described by a total potential as follows, [Sakir 1999] :

$$\Phi(x, y) = U \cdot x + \phi(x, y) \quad (1)$$

where U is the incoming uniform flow velocity and ϕ is the perturbation velocity potential which must satisfy the Laplace equation in the 2D domain. (the above conditions allow us to reduce the Navier-Stokes equations to the potential flow approximation). That is, we can write the velocity vector \mathbf{V} in terms of a scalar potential ϕ :

$$\begin{pmatrix} \mathbf{u} \\ \mathbf{v} \end{pmatrix} = \begin{pmatrix} \frac{\partial \phi}{\partial x} \\ \frac{\partial \phi}{\partial y} \end{pmatrix} \quad (2)$$

Then the continuity equation can be written as [Katz and Plotkin 2001]:

$$\nabla^2 \phi = \frac{\partial^2 \phi}{\partial x^2} + \frac{\partial^2 \phi}{\partial y^2} = 0 \quad (3)$$

Because the potential flow continuity equation is linear, the solution to potential flow problems can be built up by superimposing simple solutions.

2-1- Boundary Condition :

The corresponding boundary value problem can now be constructed by specifying boundary conditions on the total boundary S as follows :

The kinematic body boundary condition can directly specify a zero normal velocity component on the surface S_B :

$$\frac{\partial \phi}{\partial \mathbf{n}} = 0 \quad (\text{Neumann boundary condition}) \quad (4)$$

A Kutta condition should be satisfied at the trailing edge [Katz and Plotkin 2001]:

$$P_{T.E.+} = P_{T.E.-} \quad (5)$$

where $P_{T.E.+}$ and $P_{T.E.-}$ indicate the pressure values at the upper and lower side of the trailing edge, respectively.

Kutta condition states that the pressure above and below the airfoil trailing edge must be equal, and that the flow must smoothly leave the trailing edge in the same direction at the upper and lower edge, see Fig. (2).

The wake surface has zero thickness and the pressure jump across S_w is zero, while there is a jump in the potential:

$$\Delta P = P^+ - P^- = 0 \quad (6)$$

$$\Delta \phi = \phi^+ - \phi^- = \Gamma \quad (7)$$

where ΔP and $\Delta\phi$ are the pressure and potential jump on the S_w , respectively, and the constant Γ is the circulation around the body, which should be determined as a part of the solution.

The bottom condition for infinite depth (on S_B) is:

$$\lim_{y \rightarrow -\infty} \nabla\phi(x, y) = 0 \tag{8}$$

No disturbances exist for far upstream, while the potential is bounded for far downstream as a radiation condition [Sakir 1999] :

$$\lim_{x \rightarrow -\infty} |\nabla\phi| \rightarrow 0 \tag{9a}$$

$$\lim_{x \rightarrow -\infty} \phi \leq \infty \tag{9b}$$

The boundary value problem defined above can be transformed into an integral equation by applying Green's theorem to boundary S and assuming a fictitious internal fluid in two-dimensional domain. The Laplace equation in terms of the velocity potential is solved for Neumann boundary condition on the airfoil with the Kutta condition being enforced at the trailing edge. The steps to arrive at a general solution are not given here but may be found in Hess (1990) or Katz and Plotkin (2001). The general solution to Eq. (3) can be constructed by a sum of source σ and doublet μ distributions placed on the boundary S_B :

$$\phi(x, y) = -\frac{1}{2\pi} \int_{\text{airfoil+wake}} \mu n \nabla(\ln r) ds + \frac{1}{2\pi} \int_{\text{airfoil}} \sigma (\ln r) ds + \phi_\infty \tag{10}$$

2-2- Neumann Boundary Condition :

In this case it is required that $\partial\phi/\partial n$ will be specified on the solid boundary S_B ,

$$\nabla(\phi + \phi_\infty) \cdot n = 0 \tag{11}$$

The boundary condition requires that the flow disturbance, due to the body's motion through the fluid, should diminish far from the body, Eq. (9).

This condition is automatically met by all the singular solutions considered here to satisfy the boundary condition in Eq.(11), directly, we use the velocity field due to the singularity distribution :

$$\nabla\phi(x, y) = -\frac{1}{2\pi} \int_{\text{airfoil+wake}} \mu \nabla \left[\frac{\partial}{\partial n} (\ln r) \right] ds + \frac{1}{2\pi} \int_{\text{airfoil}} \sigma \nabla (\ln r) ds + \nabla\phi_\infty \tag{12}$$

If the singularity distribution strengths σ and μ are known, then Eq.(12) describes the velocity field everywhere. Substitution of Eq.(12) into the boundary condition in Eq.(11) results in :

$$\nabla\phi(x, y) = \left\{ -\frac{1}{2\pi} \int_{\text{airfoil+wake}} \mu \nabla \left[\frac{\partial}{\partial n} (\ln r) \right] ds + \frac{1}{2\pi} \int_{\text{airfoil}} \sigma \nabla (\ln r) ds + \nabla\phi_{\infty} \right\} \cdot \mathbf{n} = 0 \quad (13)$$

This equation is the basis for many numerical solutions and should hold for every point on the surface S_B . The boundary condition of Eq.(13) is then specified at each of these points in terms of the unknown singularities at all the collocation points. This approach reduces the integral equation (Eq.(13)) to a set of algebraic equations. The solution at this point is not unique, and the combination of sources and doublets must be specified. This integral equation can be solved numerically, as explained in section three.

2-3- Airfoil Geometry :

Fig.(3) compares the shapes of the Airfoil I (NACA0020) and Airfoil II (NACA4412) that are presented in this paper. Where the airfoil I is a symmetrical body and airfoil II is a nonsymmetrical body. The chord of the airfoil is the segment of the x axis from 0 to 1.

The airfoil coordinates can be calculated by the following equations :

$$y_t = \frac{t}{0.2} (0.2969\sqrt{x} - 0.126x - 0.35160x^2 + 0.2843x^3 - 0.1015x^4) \quad (14)$$

$$y_c = \begin{cases} \frac{m}{p^2} (2px - x^2) & \text{for } x < p \\ \frac{m}{(1-p^2)} ((1-2p) + 2px - x^2) & \text{for } x > p \end{cases} \quad (15)$$

The complete geometry is given by $y = y_c + y_t$

where, t is the maximum thickness as a percentage of the chord, m is the maximum camber as a percentage of the chord, and p is the chord wise position of the maximum camber as a tenth of the chord. (NACA4412, $m=4\%$, $p=40\%$, and $t=12\%$).

3- Numerical Procedure :

3-1-Panel Method :

The principle of superposition can be used to develop a simple numerical method for solving the potential flow equations for flow around an airfoil. The basic solution procedure for panel

methods consists of discrediting the surface of the airfoil with flat panels, and selecting singularities to be distributed over the panels in a specified manner, but with unknown singularity-strength parameters, and the integral is approximated by an algebraic expression on each of these panels. A system of linear algebraic equations result for the unknowns at the airfoil surface, which may be solved using techniques such as Gaussian elimination to determine the singularities of each panel at the airfoil surface. A more refined discretization of a continuous singularity distribution is the element with a constant strength. In this case, only one constant (the strength of the element) is unknown and by dividing the surface into N panels and specifying the boundary conditions on each of the collocation points, N linear algebraic equations can be constructed. In this study, constant strength doublet method is used.

3-2-Constant – Strength Doublet Method:

The simplest two-dimensional panel code that can calculate the flow over thick lifting airfoils is based on the constant-strength doublet. The surface pressure distribution can be computed by [Katz and Plotkin 2001] :

3-2-1 Selection of Singularity Element :

The potential and velocity component at a point p(x,y) belong to element extended from $x_1 \rightarrow x_2$ can be expressed by [see Fig. (4)] :

$$\phi(x, y) = -\frac{\mu}{2\pi} \int_{x_1}^{x_2} \frac{y}{(x-x_0)^2 + y^2} dx_0 \quad (16)$$

$$u(x, y) = \frac{\mu}{\pi} \int_{x_1}^{x_2} \frac{(x-x_0)y}{[(x-x_0)^2 + y^2]^2} dx_0 \quad (17)$$

$$v(x, y) = -\frac{\mu}{2\pi} \int_{x_1}^{x_2} \frac{(x-x_0)^2 - y^2}{[(x-x_0)^2 + y^2]^2} dx_0 \quad (18)$$

Where the panel is based on a flat surface element.

To establish a normal-velocity boundary condition based method, the induced velocity formulas are used (the integral for Eqs.(17) and (18)), (which are equivalent to two point vortices with a strength μ at the panel edges), see Fig.(5).

$$u_p = \frac{\mu}{2\pi} \left[\frac{y}{(x-x_1)^2 + y^2} - \frac{y}{(x-x_2)^2 + y^2} \right] \text{ Panel coordinate} \quad (19)$$

$$v_p = -\frac{\mu}{2\pi} \left[\frac{x-x_1}{(x-x_1)^2 + y^2} - \frac{x-x_2}{(x-x_2)^2 + y^2} \right] \text{ Panel coordinate} \quad (20)$$

Here, the velocity components $(u, v)_p$ are in the direction of the panel local coordinates, to transform them into the directions of the x-y global coordinates, a rotation by the panel orientation angle α_i is performed such that :

$$\begin{pmatrix} u \\ v \end{pmatrix} = \begin{pmatrix} \cos \alpha_i & \sin \alpha_i \\ -\sin \alpha_i & \cos \alpha_i \end{pmatrix} \begin{pmatrix} u_p \\ v_p \end{pmatrix} \quad (21)$$

Also the coordinates of the point p must be transformed into the panel coordinate system using :

$$\begin{pmatrix} x \\ y \end{pmatrix}_p = \begin{pmatrix} \cos \alpha_i & -\sin \alpha_i \\ \sin \alpha_i & \cos \alpha_i \end{pmatrix} \begin{pmatrix} x - x_o \\ y - y_o \end{pmatrix} \quad (22)$$

where (x_o, y_o) are the coordinates of the panel origin in the global coordinate system x-y and the subscript p stands for panel coordinates.

3-2-2 Discretization of Geometry:

Involving thick airfoils, a more dense paneling is used near the leading and trailing edges by dividing the chord line using [see Fig. (6)] :

$$x = \frac{c}{2} \left[1 - \cos \left(\frac{(i-1)\pi}{N-1} \right) \right] \quad i = 1, \dots, N \quad (23)$$

where N is the panels numbers with strength σ_j . Each panel is of single collection point placed at the center of each panel of coordinates $(x_{i=1}, y_{i=1}), (x_{i=2}, y_{i=2}), \dots, (x_{i=N}, y_{i=N})$. The normal n_i and tangential t_i to each collection point is found from the surface shape $\eta(x)$, as shown in Fig.(7).

$$n_i = \frac{\begin{pmatrix} -\frac{d\eta}{dx} \\ 1 \end{pmatrix}}{\sqrt{\left(\frac{d\eta}{dx}\right)^2 + 1}} = (\sin \alpha_i, \cos \alpha_i) \quad (24)$$

$$t_i = (\cos \alpha_i, -\sin \alpha_i) \quad (25)$$

where the angle α_i is defined as shown in Fig.(7).

However, in this lifting case, a wake panel shown in Fig.(8) has to be specified. This doublet element will have a strength μ_w and extends to $x = \infty$. In practice, the far portion (starting vortex) of the wake will have no influence and can be placed far down stream (e.g. at $(\infty, 0)$).

3-2-3 Influence Coefficients :

The free stream velocity in PANEL is assumed to be unity, since the inviscid solution in coefficient form is independent of scale. The normal velocity component at a collocation point is a combination of the velocity induced by the (jth) element at this collocation point and the free-stream velocity.

$$(u, v) \cdot n + (U_\infty, V_\infty) \cdot n = 0 \quad \text{on airfoil surface} \quad (26)$$

The free-stream contribution is known and will be transferred to the right-hand side (RHS) of the boundary condition. Consequently, the contribution of a unit strength singularity element j at collocation point1 is :

$$a_{1j} = (u, v)_{1j} \cdot n_1 \quad (27)$$

The normal velocity component at the (ith) panel is found by rotating the velocity induced by a unit strength j element by $(\alpha_j - \alpha_i)$; therefore :

$$a_{1j} = [-\sin(\alpha_j - \alpha_i), \cos(\alpha_j - \alpha_i)] \begin{pmatrix} u_{1j} \\ v_{1j} \end{pmatrix}_p \quad (28)$$

Where α_1 and α_j are the first and the (jth) panel angles.

The free-stream normal velocity component is transferred to the right-hand side. Using the formulation of Eq.(24) for the normal vector, the *RHS* becomes :

$$RHS_i = -Q_\infty (\cos \alpha \sin \alpha_i + \sin \alpha \cos \alpha_i) \quad (29)$$

3-2-4 Solve Equations:

Specifying the boundary condition of Eq.(26) for each $(i = 1 \rightarrow N)$ of the collocation points results in a set of algebraic equations with the unknown $\mu_j (j = 1 \rightarrow N)$. By applying the Kutta condition that the circulation at the trailing edge is zero requires the addition of a wake panel that will cancel this vortex:

$$(\mu_1 - \mu_N) + \mu_w = 0 \quad (30)$$

A combination of this equation with the N boundary conditions results in $N+1$ linear equations:

$$\begin{pmatrix} a_{11} & a_{12} & \dots & \dots & a_N & a_{1W} \\ a_{21} & a_{22} & \dots & \dots & a_N & a_{2W} \\ \dots & \dots & \dots & \dots & \dots & \dots \\ a_{N1} & a_{N2} & \dots & \dots & a_{NN} & a_{NW} \\ 1 & 0 & 0 & \dots & -1 & 1 \end{pmatrix} \begin{pmatrix} \mu_1 \\ \mu_2 \\ \dots \\ \mu_N \\ \mu_W \end{pmatrix} = \begin{pmatrix} RHS_1 \\ RHS_2 \\ \dots \\ RHS_N \\ 0 \end{pmatrix}$$

This system of equations is solved using Gaussian elimination to determine the singularities of each panel at the airfoil surface. A Fortran 95 language program was developed to execute all the calculations steps.

4- Calculation of Pressure, Lift, Pitching moment, and Drag coefficients :

In incompressible potential flow, The pressure coefficient can now be computed by using Bernoulli's equation such that :

$$C_p = \frac{p - p_\infty}{\frac{1}{2} \rho Q_\infty^2} \tag{31}$$

Where ρ , Q , and p are the density, speed and pressure at a point in the flow field, and the subscript ∞ refers to conditions far from the airfoil.

Combining Bernoulli's equation and the definition for the pressure coefficient yields a simple equation for the pressure coefficient in terms of the local speed of the fluid [Richard 2000]:

$$C_p = 1 - \frac{Q_t^2}{Q_\infty^2} \tag{32}$$

The lift force per unit length on an airfoil can be related to the circulation around the airfoil by the Kutta Joukowski theorem $L = \rho Q_\infty \Gamma$. The dimensionless measure for lift on an airfoil is the two-dimensional lift coefficient [Kopac, Yilmaz, and Gultop 2005] :

$$C_L = \frac{L}{\frac{1}{2} \rho Q_\infty^2 c} \tag{33}$$

The pitching moment of an airfoil is the net moment exerted on the airfoil by the flow. This is generally measured around the quarter-chord (25% of chord behind the leading edge). The moment coefficient is the non-dimensional version of the pitching moment [Sabersky 1999]:

$$C_M = \frac{M}{\frac{1}{2}\rho c^2 Q_\infty^2} \quad (34)$$

The two-dimensional drag coefficient is :

$$C_D = \frac{D}{\frac{1}{2}\rho Q_\infty^2 c} \quad (35)$$

Also, The drag coefficient found by integrating the pressures over the airfoil. The integral is approximated by considering the pressure coefficient constant over each panel, computing the contribution to drag of each panel, and summing the results.

5- Results and Discussion :

In this study the sensitivity of the solution to the number of panels is checked firstly by comparing the lift coefficient with increasing numbers of panels .Fig.(9) show the comparing of the lift coefficient with numbers of panels, Increasing the number of panels leads to increases the accuracy. The results indicates that (100) panels (50 upper, 50 lower) should be enough panels to get a stable solution. Fig.(10) represents the comparison between the lift coefficients results for NACA4412 with experimental data from Abbott and von Doenhof (1959). Agreement is good at low angles of attack, where the flow is fully attached. The agreement deteriorates as the angle of attack increases, and viscous effects start to show up as a reduction in lift with increasing angle of attack, until, finally, the airfoil stalls. The inviscid solutions from Panel method cannot capture this part of the physics. Stall occurs gradually as the separation point moves forward on the airfoil with increasing incidence. The uncambered airfoil stalls due to a sudden separation at the leading edge.

Also Fig.(11) shows a good agreement of a comparison between our results for NACA0020 with that reported by Kopac, Yilmaz, and Gultop (2005).

Figs. (12 to 17) show the streamlines of flow around the two types shape of airfoil (Airfoil I & Airfoil II) for several values of angle of attack ($\alpha = 0^\circ, 5^\circ, \text{ and } 10^\circ$) at free stream velocity ($Q_\infty=1$). Fig. (12) shows no lift is generated on the airfoil I for $\alpha = 0$ because of the symmetric fluid flow but Fig. (15) shows generating a lift on the airfoil II for $\alpha = 0$ because of the nonsymmetrical fluid flow. As the angle of attack increases as shown in Figs. (13, 14, 16, and 17) lead to more generation of lift on airfoils. The above figures show streamlines meeting at the trailing edge of the airfoils , indicating the Kutta condition is satisfied.

Also, the above figures show the convergence of streamlines near the stagnation point because ($\psi = 0$) will divided the flow to two parts for upper and lower surfaces. At very far region

from training edge the streamlines recover it is original path. Since the airfoil effects vanishing as the streamlines approaches the airfoil surface it is shape converges to the airfoil shape.

Also, by using Panel method we now have a means of easily examining the pressure distribution for different airfoil shapes. Fig. (18 to 20) show effect of angle of attack on the pressure distribution for airfoil I (NACA0020). As shown in Fig. (18) when $\alpha = 0^\circ$ case produces a mild expansion around the leading edge followed by a monotonic recovery to the trailing edge pressure. As the angle of attack increases as shown in Figs. (19 and 20) the pressure begins to expand rapidly around the leading edge, reaching a very low pressure, and resulting in an increasingly steep pressure recovery at the leading edge. This can be examine when studying airfoil pressure distributions using the NACA 0020 airfoil at 0° and 5° angles of attack as typical in Fig. (24).

Fig. (21 to 23) show effect of angle of attack on the pressure distribution for airfoil II (NACA4412). Clearly the camber (NACA4412) airfoil produces a larger disturbance, and hence a lower minimum pressure. However, this airfoil produces a milder expansion around the leading edge and a recompression extending further upstream than the airfoils I, especially at the trailing edge. As shown in Fig. (22 & 23) the values of pressure coefficient increase as angle of attack increases. The role of airfoil II (camber airfoil) in obtaining lift without producing a leading edge expansion followed by a rapid recompression immediately behind the expansion. This reduces the possibility of leading edge separation. Also Fig. (25) show the comparison between pressure distribution at 0° and 5° angles of attack for NACA4412 airfoil.

A comparison of the airfoil I and airfoil II pressure distributions at the same angle of attack is presented in Figs. (26 to 28). As the lift increases, the camber effects start to be dominated by the angle of attack effects, and the dramatic effects of camber are diminished until at a lift coefficient of 1.81 the pressure distributions start to look similar.

Fig. (29) represents the relation between the angle of attack and lift coefficient for airfoil I and airfoil II. As shown in this figure the lift coefficient will increase as the angle of attack increase.

Fig. (30) shows the pitching moment (about the quarter chord point) for the two airfoils. The uncambered NACA0020 data shows nearly zero pitching moment until flow separation starts to occur. The cambered NACA 4412 shows a significant pitching moment, and a trend due to viscous effects.

Finally, Fig.(31) shows the relation between the angle of attack and drag coefficient. As shown in the figure the drag arises from skin friction effects, further additional form drag due to the small change of pressure on the airfoil due to the boundary layer (which primarily prevents full pressure recovery at the trailing edge), and drag due to increasing viscous effects with increasing angle of attack.

6- Conclusions :

The main conclusions of the present study are :

- 1- The pressure coefficient of upper surface is higher than that of the lower surface. Also the pressure coefficient increases as the angle of attack increases.
- 2- The lift coefficient will increase as the angle of attack is increased but no lift is generated on the airfoil I (NACA0020) for $\alpha=0$ because of the symmetric fluid flow. The stream will act on the airfoil and produce a pressure difference around this airfoil.
- 3- The value of lift coefficient for airfoil II (NACA4412) is always higher than that for airfoil I, because of the airfoil geometry. Where the value of lift coefficient for airfoil I at ($\alpha=0$) is equal to (zero), but its value for airfoil II is equal to (0.523).

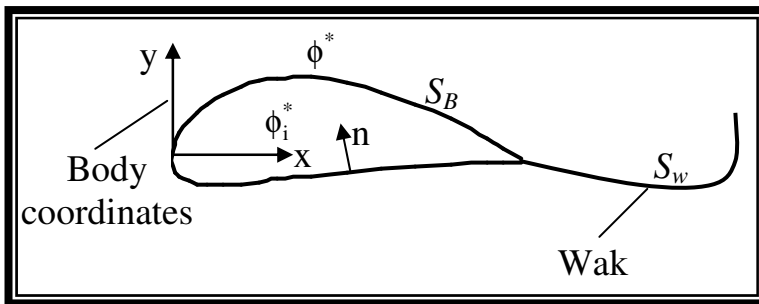


Fig.(1) Potential flow over a closed body .

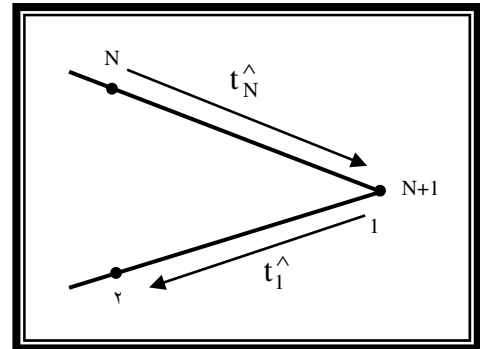


Fig.(2)Trailing edge panel nomenclature.

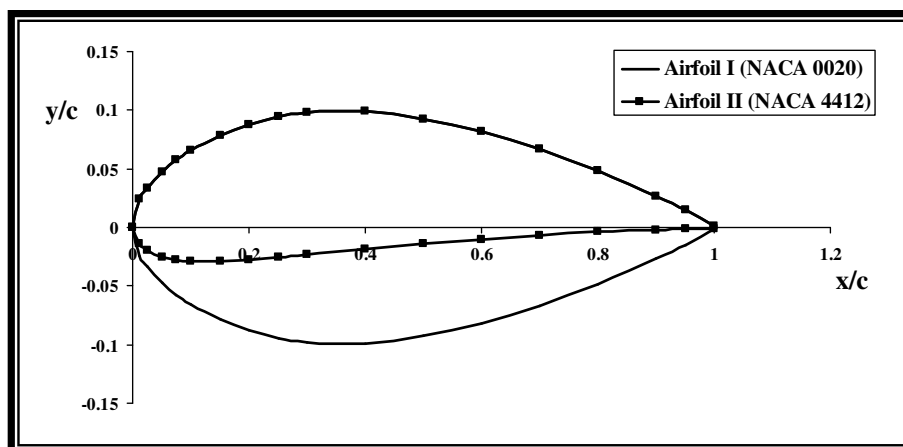


Fig.(3) Comparison of uncambered and cambered airfoils

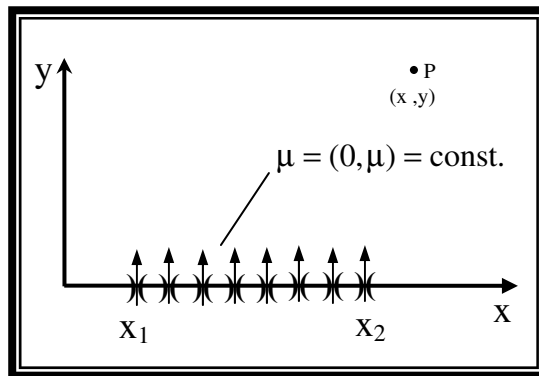


Fig.(4) Constant-strength doublet distribution along the x-axis .

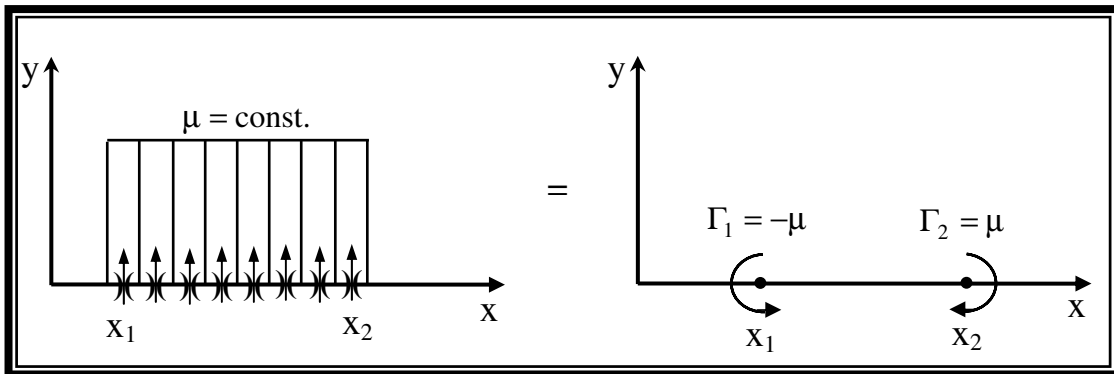


Fig.(5) Equivalence between a constant-strength doublet panel and two point vortices at the edge of the panel .

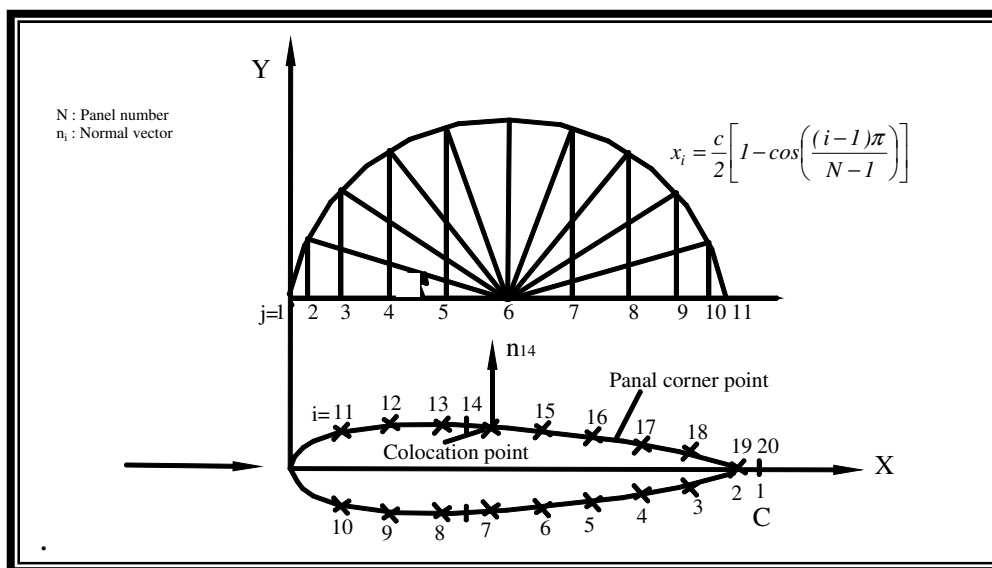


Fig.(6) Method of spacing the panels on the air foil's surface.

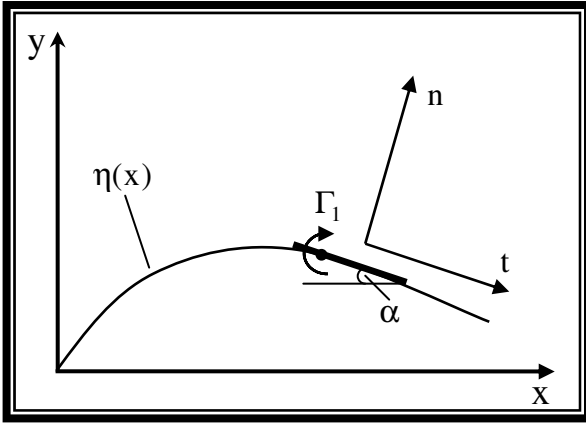


Fig.(7) Nomenclature used in defining the geometry of constant-strength singularity

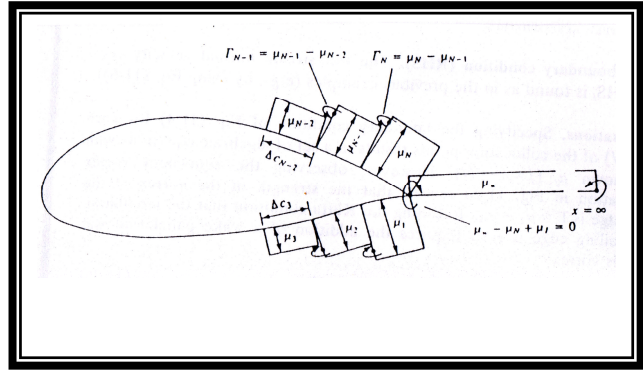


Fig.(8) Schematic description of constant strength doublet near an air foil's trailing edge .

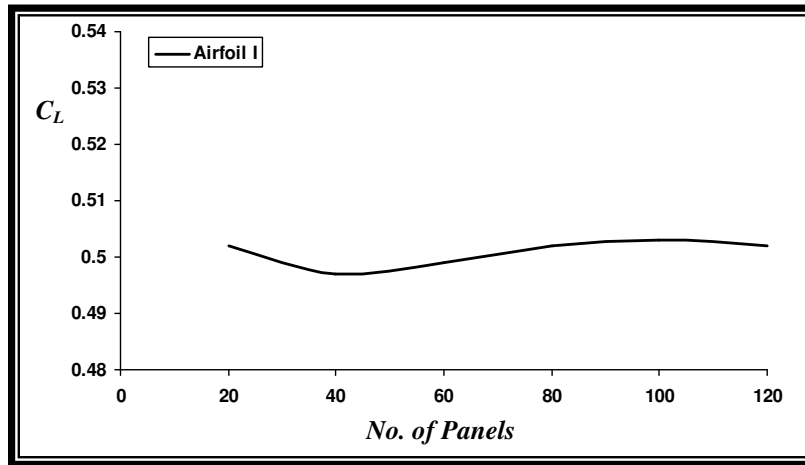


Fig.(9) Change of lift coefficient with number of panels at angle of attack = 5 degree.

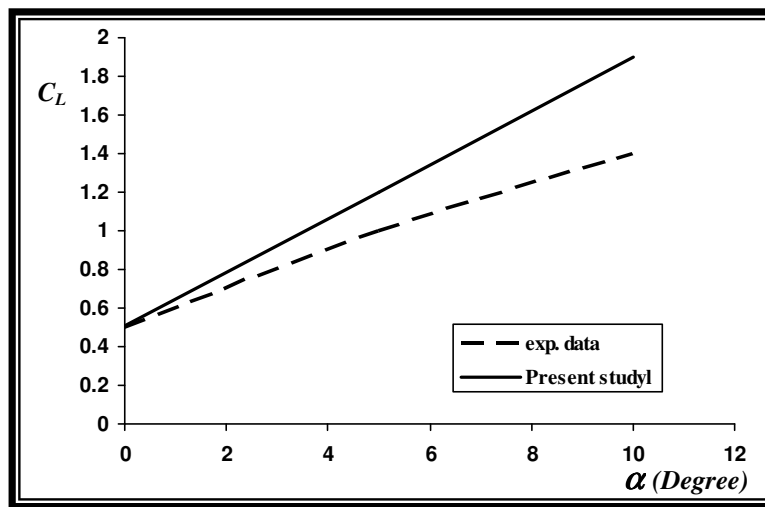


Fig.(10) Comparison of lift coefficient of this study with experimental data, by (Abbott and von Doenhof 1959) for airfoil II.

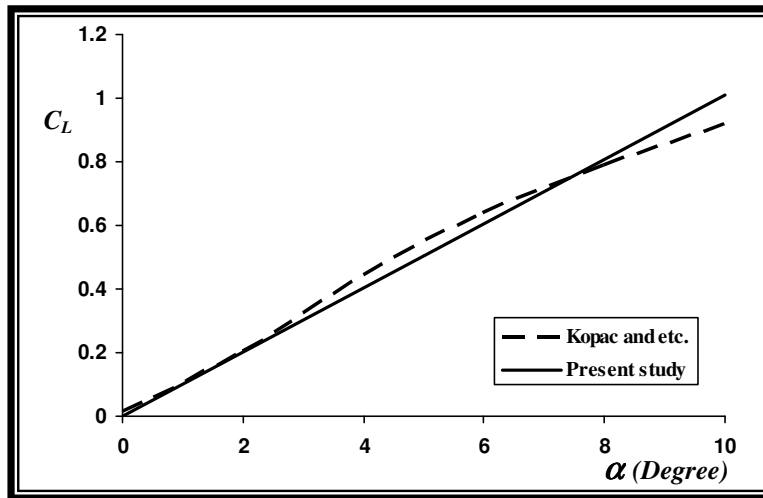
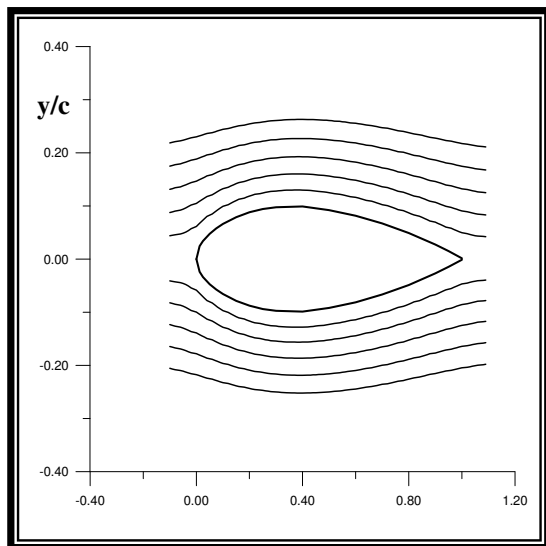
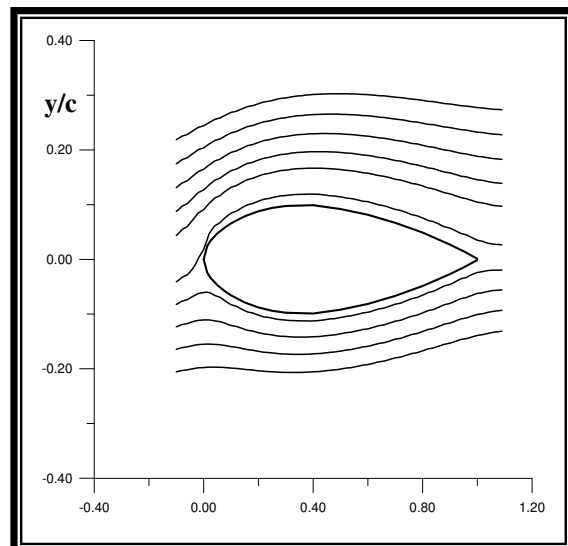


Fig.(11) Comparison of lift coefficient of this study with that of (Kopac, Yilmaz, and Gultop 2005) for airfoil I.



x/c

Fig.(12) Streamlines of flow around airfoil I at angle of attack = 0 degree . 100 Panels



x/c

Fig. (13) Streamlines of flow around airfoil I at angle of attack = 5 degree. 100 Panels

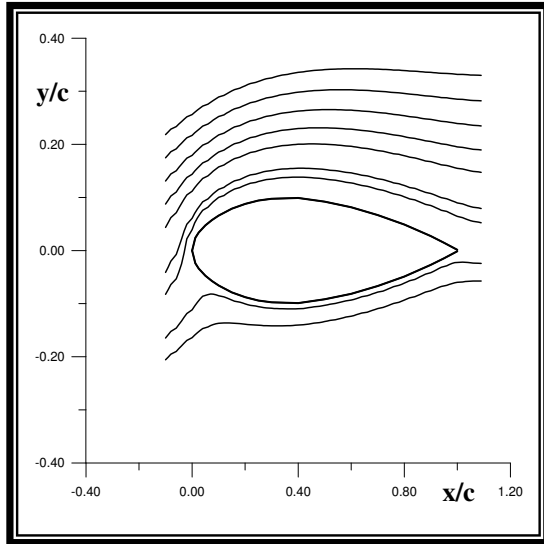


Fig.(14) Streamlines of flow around airfoil I at angle of attack = 10 degree. 100 Panels

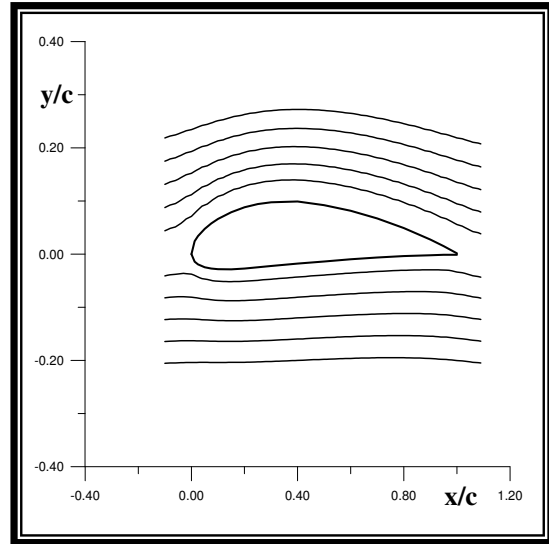


Fig.(15) Streamlines of flow around airfoil II at angle of attack = 0 degree. 100 Panels

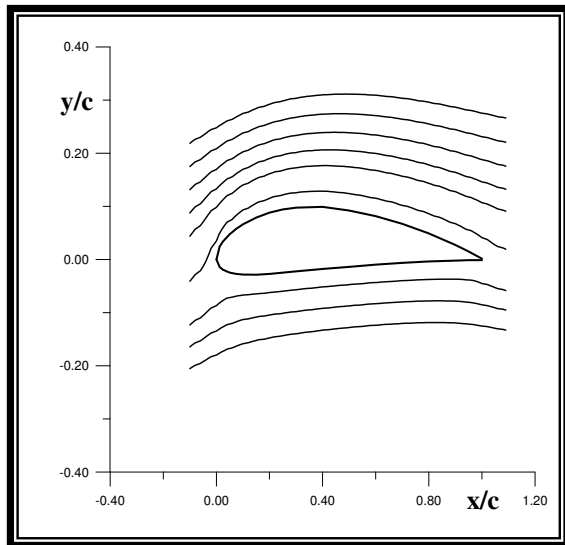


Fig. (16) Streamlines of flow around airfoil II at angle of attack = 5 degree. 100 Panels

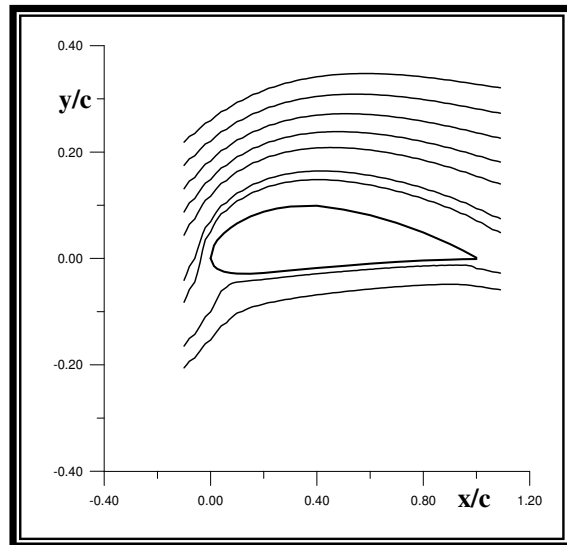


Fig. (17) Streamlines of flow around airfoil II at angle of attack = 10 degree. 100 Panels

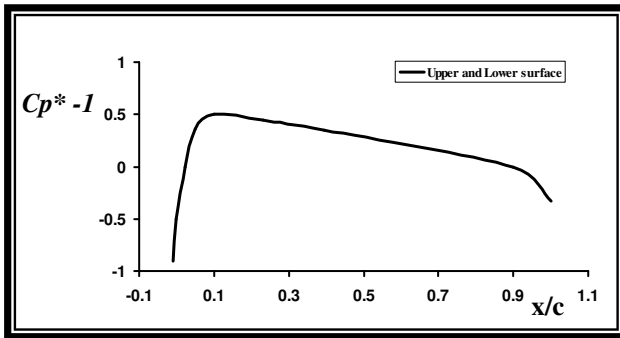


Fig. (18) Chord wise pressure distribution around airfoil I at angle of attack = 0 degree.

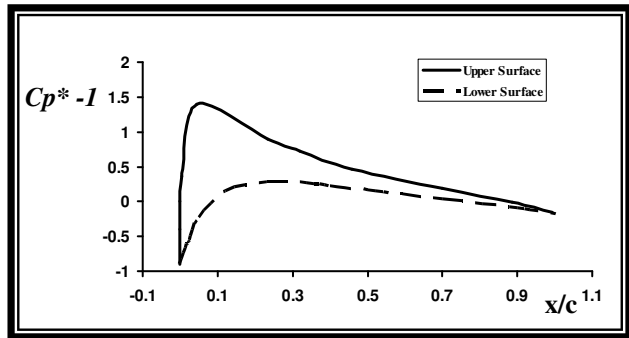


Fig. (19) Chord wise pressure distribution around airfoil I at angle of attack = 5 degree.

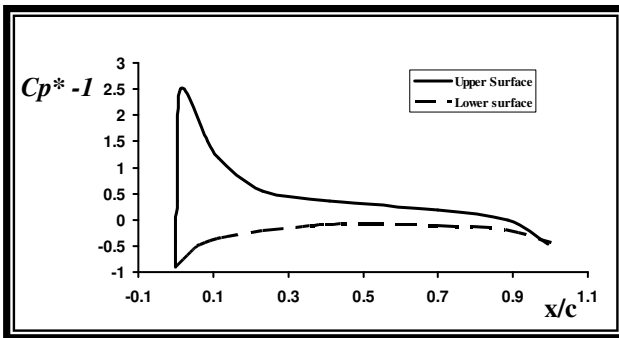


Fig. (20) Chord wise pressure distribution around airfoil I at angle of attack = 10 degree.

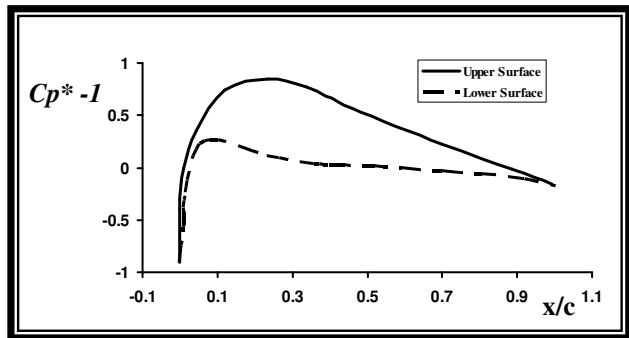


Fig. (21) Chord wise pressure distribution around airfoil II at angle of attack = 0 degree.

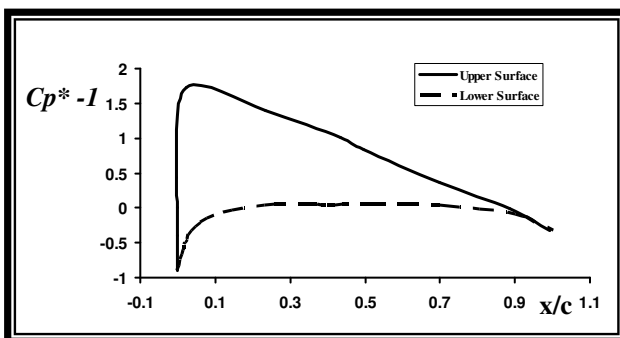


Fig. (22) Chord wise pressure distribution around airfoil II at angle of attack = 5 degree.

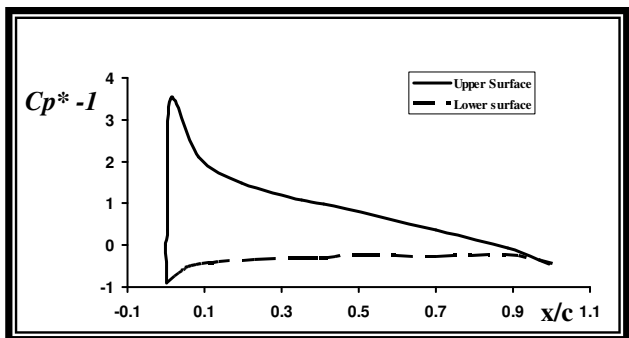


Fig. (23) Chord wise pressure distribution around airfoil II at angle of attack = 10 degree.

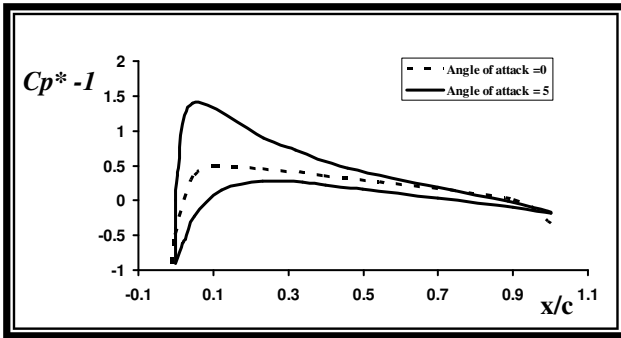


Fig. (24) Effect of angle of attack on the pressure distribution for airfoil I.

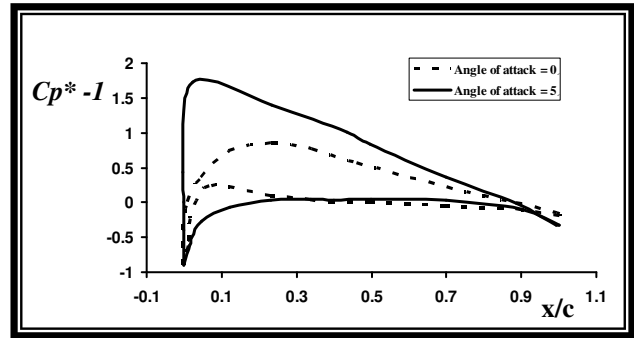


Fig. (25) Effect of angle of attack on the pressure distribution for airfoil II.

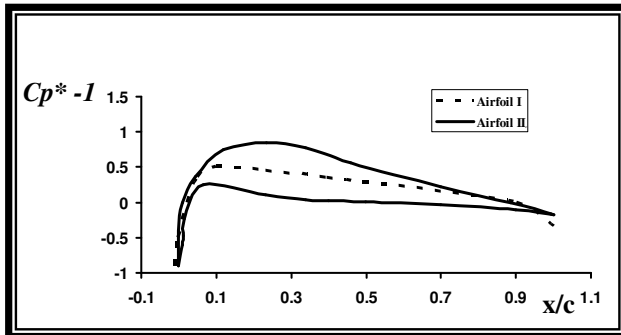


Fig. (26) Effect of airfoil shape on the pressure distribution at angle of attack = 0 degree.

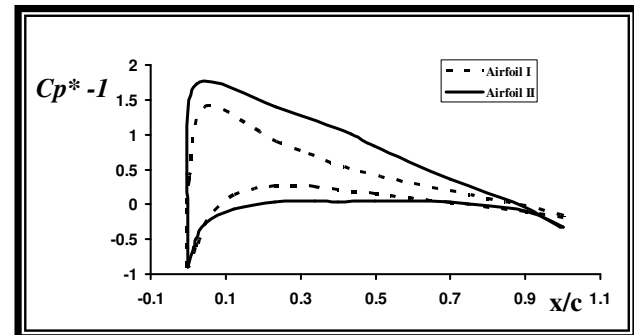


Fig. (27) Effect of airfoil shape on the pressure distribution at angle of attack = 5 degree.

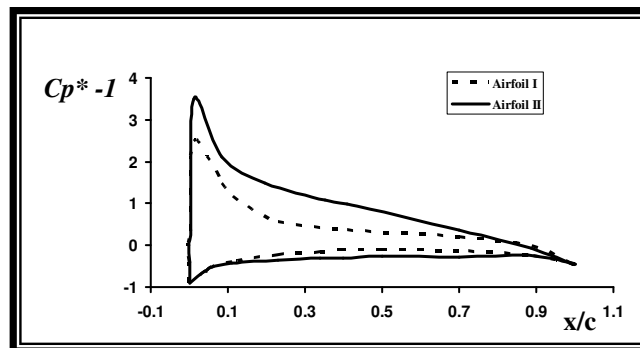


Fig. (28) Effect of airfoil shape on the pressure distribution at angle of attack = 10 degree.

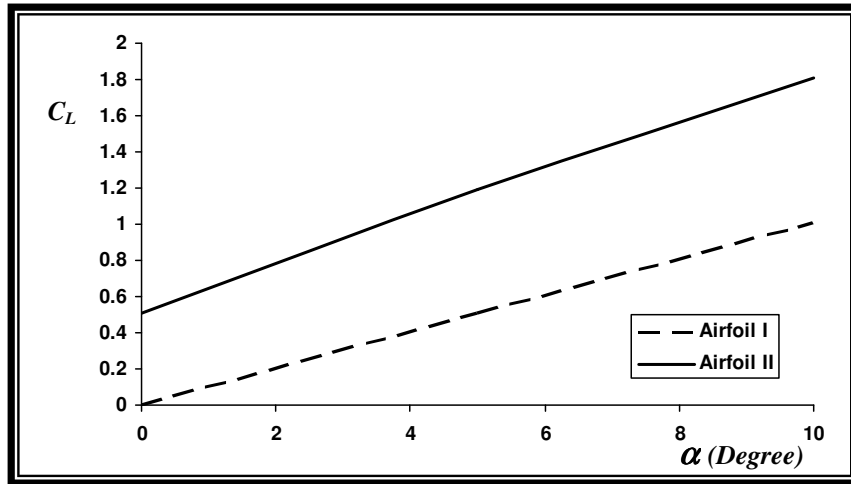


Fig. (29) The effect of the angle of attack on lift coefficient

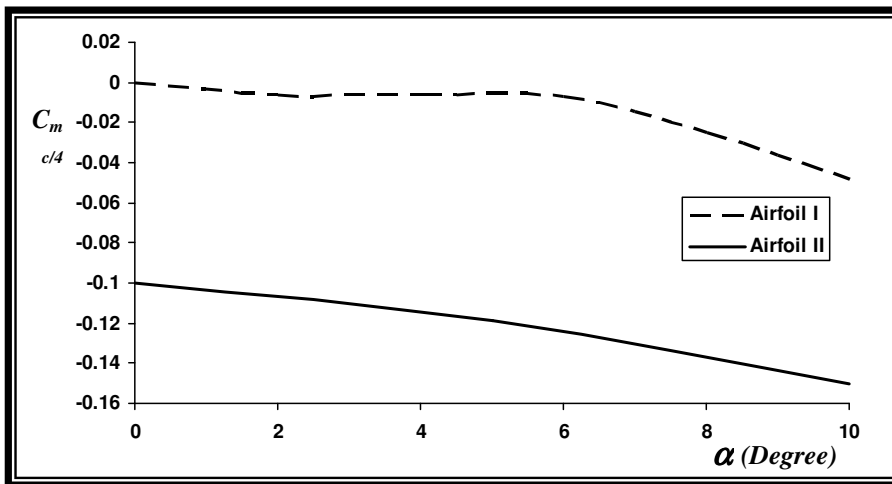


Fig. (30) The effect of the angle of attack on pitching moment

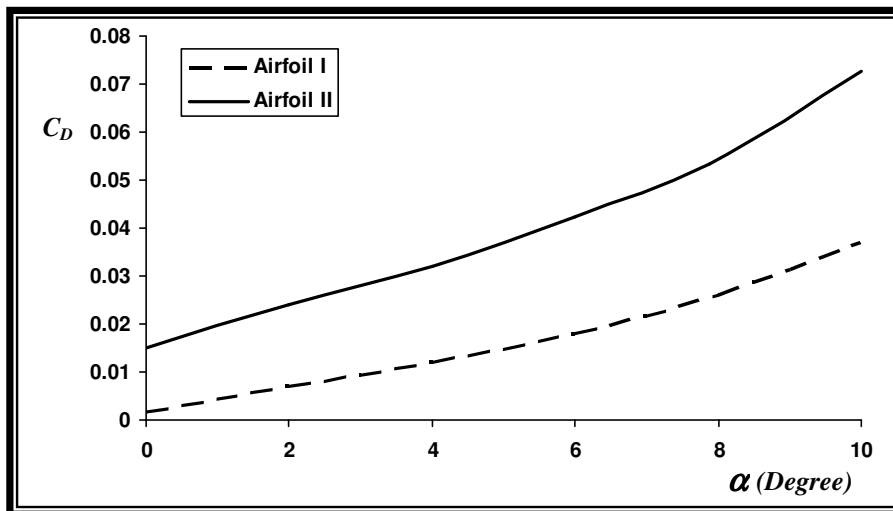


Fig. (31) The effect of the angle of attack on drag coefficient

References :

- Albano, E. and Rodden, W.P., "A Doublet lattice Method for Calculating Lift Distribution on Oscillating Surfaces in Subsonic Flows", *AIAA Journal*, Vol. 7, No.2, 1991.
- Al-baldiwe, I.A., "Approximate Aerodynamic Theory for Low Aspect Ratio Wing Body Combinations", Ph. D. Thesis, University of Technology, Iraq, 1997.
- Anderson, John P., Jr., "Modern Compressible Flow", 2nd Ed., McGraw-Hill, New York, 1990.
- Asfar, K.R., Mook, D.T., and Nayfeh, A.H., "Application of the Vortex lattice Technique to Arbitrary Bodies", *Journal of Aircraft*, vol. 16, No. 7, 1979.
- Aimen R. N., "The use of Panel method in the predication of the potential flow around two-dimensional configurations", M. Sc. Thesis, University of Babylon April 2001.
- Book, chapter four, "Incompressible Potential Flow Using Panel Methods", www.aoe.vt.edu/~mason/Mason_f/CAtxtChap4.pdf
- Chen, D.R. and Sheu, M.J., "Investigation of Internal Singularity Methods for Multielement Airfoils", *Journal of aircraft*, vol.26, No. 2, pp.189-192, 1989.
- E. Martensen, "The calculation of the pressure distribution on a cascade of thick airfoils by means of fredholm integral equation of the second kind", NASA TTF, 1971.
- Hess, J. L., "Higher Order Numerical Solution of the Integral Equation for the Two-dimensional Neumann Problem", *Computer Methods in Applied Mechanics and engineering*, vol. 2, 1991.
- Hess, J. L., "Panel Methods in Computational Fluid Dynamics", *Annual Review of Fluid Mechanics*, vol. 22, pp. 255-274, 1990.
- I.H. Abbott and A.E. Von Doenhoff, "Theory of wing sections", Dover Publications Inc, New York, 1959.
- J. L. Hess and A. M. Smith, "Calculation of non lifting potential flow about arbitrary three dimensional bodies", *Journal of Ship Research*, 1964.
- Katz, J. and Plotkin, A., "Low Speed Aerodynamics From Wing Theory To Panel Methods", McGraw-Hill Inc., New York, 2001.
- M. Kopac, M. Yilmaz, and T. Gultop, "An Investigation of the Effect of Aspect Ratio on the Airfoil Performance", *American Journal of Applied Science*2 (2): pp.545-549, 2005.
- Morino, L., Chen, L.T., and Suci, E.O., "Steady and Oscillatory Subsonic and Supersonic Aerodynamics around Complex Configuration", *AIAA Journal*, Vol. 13, No. 3, March 1975.
- Morse, P.M., Feshbach, H., "Methods of Theoretical Physics", McGraw-Hill Book Company, 1953.
- R. I. Lewis, "Vortex Element Methods for Fluid Dynamical Analysis of Engineering Systems", Cambridge University Press, 1991.
- Richard L., "Airfoil Aerodynamics Using Panel Methods", www.mae.ufl.edu/~rlf/papers/airfoil.pdf.
- Raj, P. and Gray, R., "Computation of Two dimensional Potential Flow Using Elementary Vortex Distributions", *Journal of Aircraft*, vol. 15, No.8, 1978.
- S. A. Yon, "Systematic formulation and analysis of 2-d panel methods", Master's thesis, San Diego State University, 1990.
- Sakir B., "A Panel Method for the Potential Flow Around 2-D Hydrofoils", *Tr. J. of Engineering and Environmental Science* 23 (1999) , PP. 349 - 361.
- Sabersky, R.H., Acosta, A.J., Hauptmann, E.G., Gates, E.M., "Fluid Flow", 4th ed., Prentice Hall, 1999.